$Pr_4Mo_9O_{18}$, an Atypical, Novel, Ternary Reduced Molybdenum Oxide Containing Unusual Mo_7, Mo_{13}, and Mo_{19} Clusters. Synthesis, Crystal Structure, and Physical Properties

J. Tortelier and P. Gougeon*

Université de Rennes I, Laboratoire de Chimie du Solide et Inorganique Moléculaire, UMR No. 6511, Avenue du Général Leclerc, 35042 Rennes Cedex, France

Received May 4, 1998

We present here the synthesis, crystal structure, and magnetic and resistivity studies of a remarkable ternary reduced molybdenum oxide $Pr_4Mo_9O_{18}$. Its structure was determined on single crystal by X-ray diffraction in the space group $R3m$ ($a_h = 11.3600(7)$ Å, $c_h = 50.392(8)$ Å, $V_h = 5631.8(9)$ Å^3, $Z_h = 15$; $a_{rh} = 18.032(1)$ Å, $\alpha_{rh} = 36.720(3)°$). The crystal stucture contains, in addition to the common triangular Mo_3 cluster, the new Mo_7, Mo_{13}, and Mo_{19} clusters. Contrary to the previous high-nuclearity molybdenum clusters, the Mo_{13} and Mo_{19} present hemispherical and spherical geometries, respectively, while the Mo_7 is planar. These four clusters with their oxygen environments form three different slabs parallel to the *ab* plane. The first slab is composed of Mo_3 and Mo_7 clusters in equal proportions. An infinite metallic plane based on connected Mo_3 and Mo_{13} clusters forms the second slab. The Mo_{13} aggregate presents a hemispherical geometry and results from the cis-edge-sharing of three Mo_6 octahedra having one apex in common. The last slab is based on large spherical Mo_{19} clusters that result from the hexagonal-face-sharing of two inverse Mo_{13} clusters. This extensive condensation of six Mo_6 octahedra leads to an fcc close-packed arrangement of the Mo atoms within the Mo_{19} cluster. Over the whole structure, Mo−Mo bond lengths range from 2.520(2) to 2.860(2) Å and the Mo−O bond lengths from 1.962(9) to 2.250(9) Å as usually observed in reduced molybdenum oxides. Some of the rare-earths also form a slab while the remainder are located between the Mo cluster units. The Pr−O distances range from 2.215(4) to 3.102(8) Å. Resistivity measurements on a single crystal show that $Pr_4Mo_9O_{18}$ is a small band gap semiconductor and magnetic susceptibility studies are in agreement with the presence of Pr^{3+} ions.

Introduction

Solid-state compounds in which the molybdenum is present in low formal oxidation states are generally characterized by metal−metal bondings which give rise to the formation of discrete clusters of diverse sizes and geometries or infinite chains. The most frequently encountered cluster is the Mo_6 octahedron observed, for example, in the ternary reduced molybdenum chalcogenides $M_xMo_6X_8$[1] (M = Na, K, Ca, Sr, Ba, 3d, rare-earth, Sn, Pb, ...; X = S, Se, Te). The condensation of Mo_6 clusters which can occur either via uniaxial face- or edge-sharing leads to larger columnar clusters and by extension to infinite chains. The former process is observed when the Mo_6 clusters are face-bridged by the ligands (S, Se, and Te) and is exemplified by the series of compounds $M_{n-2}Mo_{3n}X_{3n+2}$ (M = Rb, Cs; X = S, Se or Te; n = 3, 4, 5, 6, 7, 8, 10) containing Mo_9,[2] Mo_{12},[3] Mo_{15},[4] Mo_{18},[5] Mo_{21},[6] Mo_{24},[7] and Mo_{30}[7] clusters. The final stage of this face-sharing condensation is the infinite $|Mo_{6/2}|^1_\infty$ chain found in the quasi-one-dimensional compounds $M_2Mo_6X_6$ (M = Na, K, Rb, Cs; X = S, Se, Te)[8] and $AgMo_6Te_6$.[9] The edge-sharing condensation of Mo_6 octahedra is observed in the reduced molybdenum oxides where the Mo_6 clusters are edge-bridged by the oxygens. This process leads to bi-,[10] tri-,[11] tetra-,[12] and penta-octahedral[13] oligomers that are observed for example in the series $M_{n-x}Mo_{4n+2}O_{6n+4}$ (n = 2, 3, 4, 5). The ultimate step of the edge-sharing-condensation process corresponds to the infinite $|Mo_2Mo_{4/2}|^1_\infty$ chain of trans-edge-sharing Mo_6 octahedra that was first observed in $NaMo_4O_6$[14] and subsequently in the isostructural $M_xMo_4O_6$ (M = K,[15] Ba,[16] In,[17] Sn,[18] Pb[19]) compounds. Apart from these, only four other structure-types containing similar chains have been discovered: $Sc_{0.75}Zn_{1.25}Mo_4O_7$,[20] $Mn_{1.5}$-

(1) Yvon, K. *Curr. Top. Mater. Sci.* **1979**, 3, 53.
(2) Gougeon, P.; Padiou, J.; Le Marouille, J. Y.; Potel, M.; Sergent, M. *J. Solid State Chem.* **1984**, *51*, 218.
(3) Gougeon, P.; Potel, M.; Padiou, J.; Sergent, M. *Mater. Res. Bull.* **1988**, *22*, 1087.
(4) (a) Gougeon, P.; Potel, M.; Sergent, M. *Acta Crystallogr.* **1989**, *C45*, 182. (b) Gougeon, P.; Potel, M.; Sergent, M. *Acta Crystallogr.* **1989**, *C45*, 1413.
(5) Gougeon, P.; Potel, M.; Padiou, J.; Sergent, M. *Mater. Res. Bull.* **1988**, *23*, 453.
(6) (a) Gougeon, P.; Potel, M.; Sergent, M. *Acta Crystallogr.* **1990**, *C46*, 2284. (b) Picard, S.; Gougeon, P.; Potel, M. *Acta Crystallogr.* **1997**, *C53*, 1519.
(7) Gougeon, P. Thesis, Rennes, 1984.
(8) Potel, M. Thesis, Rennes, 1981.
(9) Gougeon, P.; Potel, M.; Padiou, J.; Sergent, M. *J. Solid State Chem.* **1987**, *68*, 137.
(10) (a) Hibble, S. J.; Cheetham, A. K.; Bogle, A. R. L.; Wakerley, H. R.; Cox, D. E. *J. Am. Chem. Soc.* **1988**, *110*, 3295. (b) Dronskowski, R.; Simon, A. *Angew. Chem., Int. Ed. Engl.* **1989**, *28*, 758. (c) Gougeon, P.; Potel, M.; Sergent, M. *Acta Crystallogr.* **1990**, *C46*, 1188. (d) Gougeon, P.; Gall, P.; Sergent, M. *Acta Crystallogr.* **1991**, *C47*, 421. (e) Dronskowski, R.; Simon, A.; Mertin, W. *Z. Anorg. Allg. Chem.* **1991**, *602*, 49. (f) Gall, P.; Gougeon, P. *Acta Crystallogr.* **1994**, *C50*, 7. (g) Gall, P.; Gougeon, P. *Acta Crystallogr.* **1994**, *C50*, 1183.
(11) (a) Dronskowski, R.; Simon, A.; Mertin. W. *Z. Anorg. Allg. Chem.* **1991**, *602*, 49. (b) Dronskowski, R.; Simon, A. *Acta Chem. Scand.* **1991**, *45*, 850. (c) Schimek, G. L.; Chen, S. C.; McCarley, R. E. *Inorg. Chem.* **1995**, *34*, 6130.
(12) Schimek, G. L.; Nagaki, D. A.; McCarley, R. E. *Inorg. Chem.* **1994**, *33*, 1259.
(13) (a) Dronskowski, R.; Mattausch, H. J.; Simon, A. *Zeit. Anorg. Allg. Chem.* **1993**, *619*, 1397. (b) Schimek, G. L.; McCarley, R. E. *J. Solid State Chem.* **1994**, *113*, 345.
(14) Torardi, C. C.; McCarley, R. E. *J. Am. Chem. Soc.* **1979** *101*, 3963.

10.1021/ic980500h CCC: $15.00
Published on Web 11/13/1998

Mo_8O_{11},[17] MMo_8O_{10} (M = Li, Zn),[21] and $Ho_4Mo_4O_{11}$.[22] The crystal structure of these compounds differ from each other in the manner in which the infinite molybdenum octahedral chains are coupled through the oxygen atoms to form the lattices. Thus, whereas the molybdenum chains are parallel in $Sc_{0.75}Zn_{1.25}Mo_4O_7$, $Mn_{1.5}Mo_8O_{11}$ and $Ho_4Mo_4O_{11}$, they are crosswise in MMo_8O_{10}.

In addition to their structural interest, Mo condensed cluster compounds also show interesting physical properties. Indeed, the sulfides and selenides generally present superconducting or metal−insulator transitions at low temperature. Thus, studies of the normal and superconducting states of both $Cs_2Mo_{12}Se_{14}$ and $Rb_4Mo_{18}Se_{20}$ by measuring the conductivity and magnetization of single crystals and powder samples have shown that these compounds can be classified among the "exotic" superconductors.[23] The quasi 1-D superconductor $Tl_2Mo_6Se_6$ presents extreme type II and non-BCS behaviors. On the other hand, the anisotropy of the electronic properties in the latter compound is one of the largest ever observed in a superconductor with the ratio of the conductivities parallel and perpendicular to the infinite chains ($\sigma_{\parallel}/\sigma_{\perp}$) of about 600, and the ratio of the upper critical fields ($Hc_{2\parallel}/Hc_{2\perp}$) of about 20.[24] In reduced molybdenum oxides, diverse behavior patterns in the physical properties have been also reported. For example, in the KMo_4O_6[15b] and $R_4Mo_{18}O_{32}$[25] (R = Sm, Gd → Yb) compounds, metal−insulator transitions are observed at 50 and 90 K, respectively. The RMo_5O_8 (R = La → Gd) compounds show resistivity anomalies that could be due to charge density waves[26] and magnetic properties that are also varied, with the appearance of ferromagnetic and antiferromagnetic orders as well as spin-glass such as behavior.[27] In the RMo_8O_{14} (R = La, Ce, Pr, Nd, Sm)[28] compounds, a paramagnetic moment due to the Mo_8 clusters is observed and, at low temperatures, antiferromagnetic or ferromagnetic interactions are also found, either between clusters, or between clusters and magnetic rare-earths.[29]

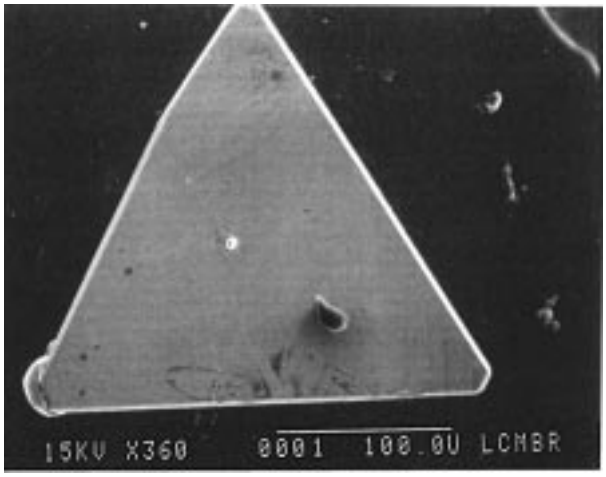

Figure 1. MEB photograph of a truncated triangular crystal of $Pr_4Mo_9O_{18}$.

We present here the crystal structure of a novel ternary reduced molybdenum oxide $Pr_4Mo_9O_{18}$ containing in addition to the common triangular Mo_3 cluster, the unusual Mo_7, Mo_{13}, and Mo_{19} clusters. Contrary to the previous high-nuclearity molybdenum clusters, the Mo_{13} and Mo_{19} present hemispherical and spherical geometries respectively whereas the Mo_7 is planar. These types of cluster geometries are new to solid-state compounds and were previously encountered only in metal−organic compounds.

Experimental Section

Crystal Growth. Starting reagents were Pr_6O_{11} (Rhône-Poulenc, 99.999%), MoO_3 (Strem Chemicals, 99.9%), and Mo (Cimebocuze, 99.9%), all in powder form. The rare-earth oxide was prefired at 1000 °C before use, and the Mo powder was heated under a hydrogen flow at 1000 °C for 6 h. The stoichiometric mixture was pressed into a ca. 5 g pellet and loaded into a molybdenum crucible (depth, 2.5 cm; diam, 1.5 cm) which was previously cleaned by heating at 1500 °C for 15 min under a dynamic vacuum of about 10^{-5} Torr and then sealed under a low argon pressure using an arc welding system. X-ray-pure powder samples and single crystals of $Pr_4Mo_9O_{18}$ were obtained by heating the charge at a rate of 300 °C/h to 1600 °C and maintained at this temperature for 48 h. The charge was then cooled at 100 °C/h down to 1100 °C and finally furnace cooled. The crystals were generally obtained as thin black truncated triangular plates reflecting the layered structure of the compound (Figure 1).

X-ray Single-Crystal Studies. A crystal of $Pr_4Mo_9O_{18}$ with approximate dimensions $0.1 \times 0.08 \times 0.04$ mm^3 was selected for data collection. The intensities of 7222 reflections (3816 unique reflections, $R_{int} = 0.038$) were collected by the $\omega-2\theta$ scan method in the 2−76° 2θ range (h, k, l range: 0/19, −19/0, 0/87) on a CAD4 Nonius diffractometer using graphite-monochromatized Mo Kα radiation (λ = 0.710 73 Å) at room temperature. Three orientation and three intensity control reflections from diverse regions of reciprocal space were checked every 250 reflections and every hour respectively and showed no systematic variations throughout data collection. The data set was corrected for Lorentz and polarization effects and for absorption (μ = 20.025 mm^{-1}) by employing the ψ scan method[30] on six reflections. The transmission factors were in the range from 0.476 to 1.00. Analysis of the data did not reveal any systematic absence. The lattice constants were determined by least-squares refinement of the setting angles of 25 reflections in the 2θ range 10−34° that had been automatically centered on the diffractometer. The crystal structure was initially solved in the R3 space group with the direct methods program SHELXS[31] and subsequent difference Fourier syntheses. At this stage,

(15) (a) Hoffman, R.; Hoppe, R.; Bauer, K.; Range, K. J. *J. Less Common Met.* **1990** *161*, 279. (b) Ramanujachary, K. V.; Greenblatt, M.; Jones, E. B.; McCarroll, W. H. *J Solid State Chem.* **1993**, *102*, 69.
(16) Torardi, C. C.; McCarley, R. E. *J. Less Common Met.* **1986** *116*, 169.
(17) McCarley, R. E.; Lii, K. H.; Edwards, P. A.; Brough, L. F. *J. Solid State Chem.* **1985**, *57*, 17.
(18) Aufdembrink, B. Ph.D. Dissertation, Iowa State University, 1985.
(19) (a) Torardi, C. C.; McCarley, R. E. *J. Solid State Chem.* **1981**, *37*, 393. (b) Wang, S. L.; Yeh, J. Y. *Acta Crystallogr.* **1991**, *B47*, 446.
(20) (a) McCarley, R. E. *Am. Chem. Soc. Symp. Ser.* **1981** *155*, 41. (b) McCarley, R. E. *Philos. Trans. R. Soc. London A* **1982** *308*, 41.
(21) Lii, K. H.; McCarley, R. E.; Kim, S.; Jacobson, R. A. *J. Solid State Chem.* **1986**, *64*, 347.
(22) Gougeon, P.; Gall, P.; McCarley, R. E. *Acta Crystallogr.* **1991**, *C47*, 1585.
(23) Brusetti, R.; Laborde, O.; Sulpice, A.; Calemczuk, R.; Potel, M.; Gougeon, P. *Phys. Rev. B* **1995**, *52*, 4481.
(24) Brusetti, R.; Monceau, P.; Potel, M.; Gougeon, P.; Sergent, M. *Solid State Commun.* **1988**, *66*, 181.
(25) Gall, P.; Gougeon, P.; Greenblatt, M.; McCarroll, W. H.; Ramanujachary, K. V. *J. Solid State Chem.* **1997**, *134*, 45.
(26) Gall, P.; Gougeon, P.; Greenblatt, M.; Jones, E. B.; McCarroll, W. H.; Ramanujachary, K. V. *Croat. Chem. Acta* **1995**, *68*, 849 (special issue, Metal Clusters: Theory and Experiment).
(27) Gall, P.; Noël, H.; Gougeon, P. *Mater. Res. Bull.* **1993**, *28*, 1225.
(28) (a) Leligny, H.; Ledésert, M.; Labbé, Ph.; Raveau, B.; McCarroll, W. H. *J. Solid State Chem.* **1990**, *87*, 35−43. (b) Gougeon, P.; McCarley, R. E. *Acta Crystallogr.* **1991**, *C47*, 241. (c) Leligny, H.; Labbé, Ph.; Ledesert, M.; Hervieu, M.; Raveau, B; McCarroll, W. H. *Acta Crystallogr.* **1993**, *B49*, 444−454. (d) Kerihuel, G.; Gougeon, P. *Acta Crystallogr.* **1995**, *C51*, 787. (e) Kerihuel, G.; Gougeon, P. *Acta Crystallogr.* **1995**, *C51*, 1475. (f) Kerihuel, G.; Tortelier, J.; Gougeon, P. *Acta Crystallogr.* **1996**, *C52*, 2389. (g) Tortelier, J.; Gougeon, P. *Acta Crystallogr.* **1997**, *C53*, 668.
(29) Gougeon, P.; Kerihuel, G.; Noël, H.; Greedan, J. Presented at the Vth European Conference on Solid State Chemistry, Montpellier 4−7 Septembre 1995; Abstract xx.
(30) North, A. C. T.; Phillips, D. C.; Mathews, F. S. *Acta Crystallogr.* **1968**, *A24*, 351.

Table 1. X-ray Crystallographic and Experimental Data for $Pr_4Mo_9O_{18}$

empirical formula	$Pr_4Mo_9O_{18}$
fw, g mol^{-1}	1715.10
space group	*R*3*m* (No. 160)
a_h,[a] Å	11.3600(7)
c_h, Å	50.392(8)
V_h, Å^3	5631.8(9)
Z_h	15
a_{rh},[b] Å	18.032(1)
α_{rh}, deg	36.720(2)
V_{rh}, Å^3	1877.3(2)
ρ_{calcd}, g cm^{-3}	7.585
T, °C	20
λ, Å	0.710 73 (Mo Kα)
μ, cm^{-1}	200.25
R_1[c] (on all data)	0.0282
wR_2[d] (on all data)	0.0485

[a] Hexagonal setting. [b] Rhombohedral setting. [c] $R_1 = \sum||F_o| - |F_c||/\sum|F_o|$. [d] $wR_2 = \{\sum[w(F_o^2 - F_c^2)^2]/\sum[w(F_o^2)^2]\}^{1/2}$, $w = 1/[\sigma^2(F_o^2) + (0.0173P)^2 + 7.6090P]$, where $P = [\mathrm{Max}(F_o^2,0) + 2F_c^2]/3$.

examination of the atomic coordinates clearly showed that the structure could be better described in the *R*3*m* space group. Consequently, refinements were continued in the latter space group. Full-matrix least-squares refinement on F^2 on positional and anisotropic displacement parameters for heavy atoms (Pr, Mo) and isotropic displacement parameters for oxygen atoms was carried out using SHELXL.[32] An analysis of the anisotropic parameters revealed a strong anisotropy for the Mo(3) atom ($U_{11} = U_{22} \approx 13U_{33}$) in the *a*,*b* plane. As the refinement of its occupancy factor indicated a full occupation, Mo(3) was subsequently moved from the 3*m* site (0, 0, *z*) to a 3 site [(*x*, 2*x*, *z*) = (0.0087(4), 0.0173(7), 0.67886(4)], with a third of its occupancy. The final refinement led to the values of $R(F_o) = 0.0282$, $R_w(F_o^2) = 0.0485$ and $S = 1.096$ for all independent data. The maximum shift/σ ratio for all the 217 refined parameters was less than 0.01. The secondary extinction coefficient was $4.9(2) \times 10^{-5}$ and the final electron density difference map was flat with a maximum of 2.24 e/Å^3 and minimum of −2.42 e/Å^3. An attempt to establish the absolute configuration was made by refining Flack's *x* parameter.[33] The resulting value of 0.48(2) gave evidence that the crystal studied was racemically twinned. Examination of the final model with the use of the program MYSSIM[34] in the PLATON package did not show extra symmetries. Refinements of the occupancy factors for the Pr and Mo atoms showed that the sites were all fully occupied. Calculations were performed on a Digital Pentium Celebris 590 FP for SHELXL-93 and on a Digital microVAX 3100 for the MolEN programs[35] (Data reduction and absorption corrections). The crystallographic and experimental data are summarized in Table 1. The final atomic coordinates and equivalent isotropic displacement parameters are reported in Table 2, and selected interatomic distances in Tables 3−5.

Electrical Resistivity. The ac resistivity measurement was carried out on a single crystal using a standard four-probe technique between 290 and 80 K. Ohmic contacts were made by attaching molten indium ultrasonically. The voltage drops across the sample were recorded as a function of temperature. The temperature readings were provided by platinum resistance thermometers.

Magnetic Susceptibility. Magnetic susceptibility data of $Pr_4Mo_9O_{18}$ were collected on a SHE-906 SQUID magnetosusceptometer in the temperature range 5−300 K under a magnetic field of 4 kgauss. The measurements were carried out on a cold pressed pellet (ca. 150 mg) of crushed selected crystals. Data were corrected from the diamagnetism of the sample holder prior to analysis.

(31) Sheldrick, G. M. *Acta Crystallogr.* **1990**, *A46*, 467.
(32) Sheldrick, G. M. *SHELXL93*: *Program for the Refinement of Crystal Structures*; University of Göttingen: Germany, 1993.
(33) Flack, H. D. *Acta Crystallogr.* **1983**, *A39*, 876.
(34) Le Page, Y. *J. Appl. Crystallogr.* **1987**, *20*, 264.
(35) Fair, C. K. *MolEN: An Interactive Intelligent System for Crystal Structure Analysis*; Enraf-Nonius, Delft Instruments X-ray Diffraction BV: Rontgenweg 1, 2624 BD Delft, The Netherlands, 1990.

Table 2. Positional Parameters and Equivalent Isotropic Displacement Parameters

atom	*x*	*y*	*z*	U_{eq} (Å^2)[a]
Pr(1)	0.11229(3)	0.22458(5)	0.22106(2)	0.00671(9)
Pr(2)	0.0000	0.0000	0.28229(2)	0.0087(2)
Pr(3)	−0.22031(3)	0.22031(3)	0.37949(2)	0.00796(9)
Pr(4)	0.11617(3)	0.23233(5)	0.40801(2)	0.00734(9)
Pr(5)	0.22653(2)	0.45307(5)	0.47371(2)	0.00450(8)
Pr(6)	0.0000	0.0000	0.55295(2)	0.0080(2)
Pr(7)	−0.11128(3)	0.11128(3)	0.61640(2)	0.00731(9)
Pr(8)	0.11135(3)	0.22269(5)	0.74367(2)	0.00656(8)
Mo(1)	−0.14787(8)	−0.07394(4)	0.34564(2)	0.00331(12)
Mo(2)	0.23618(6)	0.24825(6)	0.67917(2)	0.00679(10)
Mo(3)	0.0087(4)	0.0173(7)	0.67886(4)	0.0027(12)
Mo(4)	0.32496(6)	0.42388(5)	0.82401(2)	0.00303(9)
Mo(5)	0.0000	0.0000	0.15931(3)	0.0033(2)
Mo(6)	0.34075(8)	0.17037(4)	0.44738(2)	0.00335(11)
Mo(7)	−0.08116(4)	−0.16231(8)	0.11224(2)	0.00350(11)
Mo(8)	−0.07619(4)	0.07619(4)	0.48925(2)	0.00301(12)
Mo(9)	0.34421(8)	0.17210(4)	0.29644(2)	0.00352(12)
Mo(10)	0.25103(4)	0.50205(8)	0.63014(2)	0.00389(12)
Mo(11)	0.33350(7)	0.42238(5)	0.58491(2)	0.00356(7)
Mo(12)	0.0000	0.0000	0.91824(3)	0.0034(2)
Mo(13)	0.17060(4)	0.34120(8)	0.54058(2)	0.00359(12)
Mo(14)	0.08209(4)	0.16419(8)	0.87292(2)	0.00312(12)
O(1)	−0.2536(5)	−0.2502(5)	0.3680(2)	0.0070(9)
O(2)	0.3345(7)	0.1672(4)	0.6573(2)	0.0063(12)
O(3)	0.0000	0.0000	0.3748(3)	0.007(2)
O(4)	−0.0810(3)	−0.1619(7)	0.3187(2)	0.0045(11)
O(5)	0.1775(4)	0.3550(8)	0.7042(2)	0.0118(14)
O(6)	0.1621(8)	0.0811(4)	0.7065(2)	0.0103(13)
O(7)	0.3344(5)	−0.0807(5)	0.6542(1)	0.0059(8)
O(8)	0.0785(4)	−0.0785(4)	0.6511(2)	0.0062(12)
O(9)	0.0867(5)	−0.3307(5)	0.5147(1)	0.0063(9)
O(10)	−0.1683(3)	−0.3365(7)	0.5132(2)	0.0048(11)
O(11)	−0.0794(3)	−0.1588(7)	0.1861(2)	0.0033(11)
O(12)	0.0811(3)	0.1622(7)	0.5168(2)	0.0048(11)
O(13)	0.0000	0.0000	0.4620(3)	0.006(2)
O(14)	0.2535(5)	0.2624(5)	0.4685(1)	0.0054(8)
O(15)	0.1551(3)	−0.1551(3)	0.7993(2)	0.0030(10)
O(16)	−0.0961(4)	−0.1922(8)	0.4210(2)	0.0104(13)
O(17)	−0.3339(5)	−0.4192(5)	0.4207(1)	0.0066(8)
O(18)	0.0000	0.0000	0.0880(3)	0.006(2)
O(19)	0.0000	0.0000	0.9882(3)	0.005(2)
O(20)	0.2458(5)	0.2444(5)	0.2736(1)	0.0053(8)
O(21)	0.1592(4)	−0.1592(4)	0.6079(2)	0.0058(11)
O(22)	0.2446(5)	0.0003(5)	0.5627(2)	0.0069(9)
O(23)	0.5059(3)	−0.5059(3)	0.5608(2)	0.0051(11)
O(24)	0.0000	0.0000	0.8467(3)	0.006(2)
O(25)	0.0000	0.0000	0.0384(3)	0.007(2)
O(26)	0.0000	0.0000	0.2370(3)	0.004(2)
O(27)	0.0000	0.0000	0.5989(3)	0.007(2)
O(28)	0.0000	0.0000	0.7910(3)	0.012(2)
O(29)	0.2222(7)	0.1111(4)	0.7601(2)	0.0072(11)[a]

[a] U_{eq} is defined as one-third of the trace of the orthogonalizd $\mathbf{U}_{ij}$ tensor.

Results and Discussion

Description of Structure. A projection of the remarkable crystal structure of $Pr_4Mo_9O_{18}$ is represented in Figure 2. It shows that this structure can be viewed as a stacking along the *c* axis of four different slabs interconnected through oxygen atoms. The A slab is made up of molybdenum and oxygen atoms, the B slab of praseodymium and oxygen atoms, and the C and D slabs of molybdenum, praseodymium, and oxygen atoms. In the A, C, and D slabs, the molybdenum atoms form four different types of clusters: Mo_3, Mo_7, Mo_{13}, and Mo_{19}. While the Mo_3 cluster has been observed in a large number of compounds, the other three metallic clusters are totally new to inorganic chemistry. Figure 3 shows the arrangement of the four different clusters within the unit cell.

Table 3. Selected Mo−Mo Interatomic Distances (Å) for $Pr_4Mo_9O_{18}$

Slab A	
Mo_3	
Mo(1)−Mo(1)	2.520(2)
Mo_7	
Mo(2)−Mo(2)	2.546(2)
Mo(2)−Mo(3)	2.604(6)
Mo(2)−Mo(3)	2.7668(9)
Mo(2)−Mo(3)	2.900(6)
Mo(2)−Mo(2)	2.957(2)
Slab C	
Mo_{13}	
Mo(4)−Mo(4)	2.568(1)
Mo(4)−Mo(5)	2.7136(6)
Mo(4)−Mo(7)	2.7280(9)
Mo(4)−Mo(6)	2.7578(9)
Mo(4)−Mo(4)	2.853(1)
Mo(5)−Mo(7)	2.860(2)
Mo(6)−Mo(7)	2.7783(7)
Mo(6)−Mo(8)[a]	2.808(1)
Mo(7)−Mo(7)	2.766(2)
Mo_3	
Mo(8)−Mo(8)	2.597(2)
Slab D	
Mo_{19}	
Mo(9)−Mo(10)	2.7476(7)
Mo(9)−Mo(11)	2.761(1)
Mo(10)−Mo(11)	2.782(1)
Mo(10)−Mo(12)	2.796(2)
Mo(10)−Mo(10)	2.805(2)
Mo(11)−Mo(13)	2.749(1)
Mo(11)−Mo(11)	2.773(2)
Mo(11)−Mo(12)	2.7760(5)
Mo(11)−Mo(11)	2.779(2)
Mo(11)−Mo(14)	2.7864(9)
Mo(12)−Mo(14)	2.798(2)
Mo(13) −Mo(14)	2.7735(7)
Mo(14)−Mo(14)	2.798(2)

[a] Inter-cluster distances between Mo13 and Mo3 clusters.

Table 4. Selected Mo−O Interatomic Distances (Å) for $Pr_4Mo_9O_{18}$

Mo(1)−O(4) (×2)	2.046(6)	Mo(7)−O(18)	2.012(8)
Mo(1)−O(3)	2.07(1)	Mo(7)−O(17) (×2)	2.063(5)
Mo(1)−O(1) (×2)	2.079(5)	Mo(7)−O(15)	2.169(7)
Mo(1)−O(2)	2.117(8)		
		Mo(8)−O(13)	2.033(9)
Mo(2)−O(1)	2.069(5)	Mo(8)−O(12) (×2)	2.081(6)
Mo(2)−O(7)	2.074(5)	Mo(8)−O(14) (×2)	2.113(5)
Mo(2)−O(5)	2.078(7)	Mo(8)−O(10)	2.177(7)
Mo(2)−O(2)	2.083(5)		
Mo(2)−O(8)	2.104(6)	Mo(9)−O(7) (×2)	2.004(5)
Mo(2)−O(6)	2.149(6)	Mo(9)−O(20) (×2)	2.040(5)
		Mo(9)−O(4)	2.114(7)
Mo(3)−O(8)	1.962(9)		
Mo(3)−O(6) (×2)	2.061(8)	Mo(10)−O(19)	2.045(8)
Mo(3)−O(8) (×2)	2.154(8)	Mo(10)−O(7) (×2)	2.070(5)
Mo(3)−O(6)	2.250(9)	Mo(10)−O(21)	2.125(7)
		Mo(11)−O(20)	2.060(5)
Mo(4)−O(10)	2.052(5)	Mo(11)−O(21)	2.078(5)
Mo(4)−O(14)	2.088(5)	Mo(11)−O(22)	2.079(5)
Mo(4)−O(11)	2.107(6)	Mo(11)−O(23)	2.093(5)
Mo(4)−O(15)	2.110(6)		
Mo(4)−O(9)	2.129(5)	Mo(13)−O(22) (×2)	2.022(5)
		Mo(13)−O(9) (×2)	2.044(5)
Mo(5)−O(11) (×3)	2.066(7)	Mo(13)−O(12)	2.130(7)
Mo(6)−O(16)	1.975(8)		
Mo(6)−O(14) (×2)	2.059(5)	Mo(14)−O(9) (×2)	2.067(5)
Mo(6)−O(17) (×2)	2.098(5)	Mo(14)−O(23)	2.077(7)
		Mo(14)−O(24)	2.086(8)

The first slab (A in Figure 2) consists of an equal mixture of the well-known Mo_3O_{13} and the novel Mo_7O_{24} cluster units sharing part of their oxygen environment. The triangular Mo_3 cluster, included in the Mo_3O_{13} unit, was first observed in 1957 by W. H. McCarroll in $Zn_2Mo_3O_8$[36] and is one of the most studied clusters in molybdenum oxide chemistry. These studies have led to the synthesis of a whole range of compounds such as $M_2Mo_3O_8$ (M = Mg, Mn, Fe, Co, Ni, Zn, Cd),[37] $LiRMo_3O_8$

Table 5. Selected Pr−O Interatomic Distances (Å) for $Pr_4Mo_9O_{18}$

Pr(1)−O(10)	2.322(7)	Pr(5)−O(28)	2.252(5)
Pr(1)−O(26)	2.351(4)	Pr(5)−O(14) (×2)	2.349(5)
Pr(1)−O(22) (×2)	2.423(5)	Pr(5)−O(29)	2.367(7)
Pr(1)−O(11) (×2)	2.639(5)	Pr(5)−O(9) (×2)	2.513(5)
Pr(1)−O(23) (×2)	2.829(5)	Pr(5)−O(15) (×2)	2.732(5)
		Pr(5)−O(24)	2.900(9)
Pr(2)−O(26)	2.28(2)		
Pr(2)−O(4) (×3)	2.428(7)	Pr(6)−O(27)	2.32(2)
Pr(2)−O(20) (×6)	2.819(5)	Pr(6)−O(12) (×3)	2.421(7)
		Pr(6)−O(22) (×6)	2.820(5)
Pr(3)−O(25)	2.258(2)		
Pr(3)−O(1) (×2)	2.444(5)	Pr(7)−O(2)	2.336(8)
Pr(3)−O(17) (×2)	2.518(5)	Pr(7)−O(27)	2.360(5)
Pr(3)−O(5) (×2)	2.778(6)	Pr(7)−O(20) (×2)	2.462(5)
Pr(3)−O(18)	3.063(9)	Pr(7)−O(8) (×2)	2.618(5)
		Pr(7)−O(21) (×2)	2.817(5)
Pr(4)−O(16) (×2)	2.215(4)		
Pr(4)−O(29)	2.291(7)	Pr(8)−O(29) (×2)	2.340(4)
Pr(4)−O(1) (×2)	2.464(5)	Pr(8)−O(5)	2.376(9)
Pr(4)−O(3)	2.832(8)	Pr(8)−O(17) (×2)	2.440(5)
Pr(4)−O(17) (×2)	3.102(8)	Pr(8)−O(6) (×2)	2.711(6)
		Pr(8)−O(15)	2.932(7)

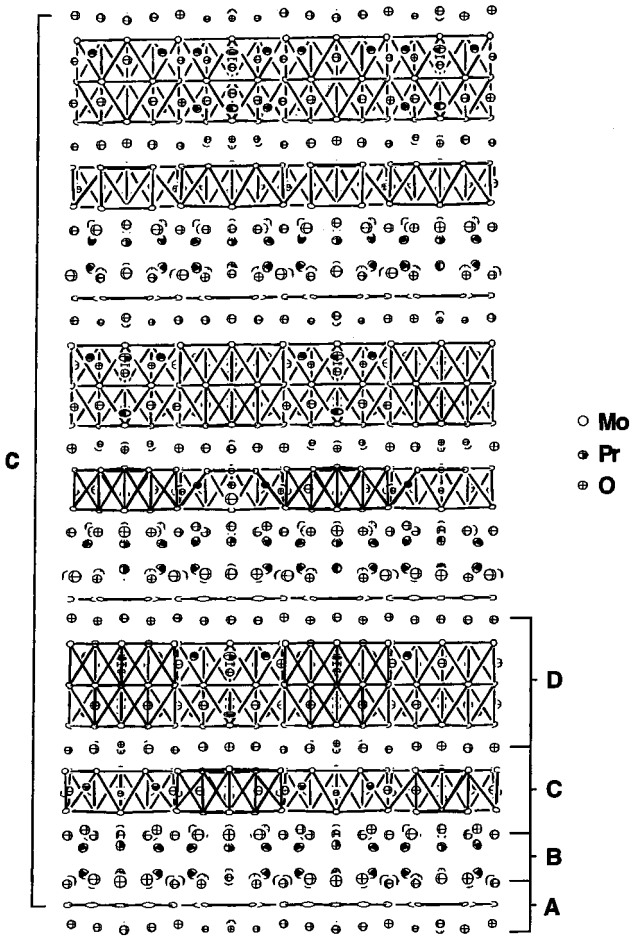

Figure 2. Projection of the crystal structure of $Pr_4Mo_9O_{18}$ along the *b* axis of the hexagonal unit cell.

(36) McCarroll, W. H.; Katz, L.; Ward, R. *J. Am. Chem. Soc.* **1957**, *79*, 5410.
(37) Le Page, Y.; Strobel, P. *Acta Crystallogr.* **1982**, *B38*, 1265.

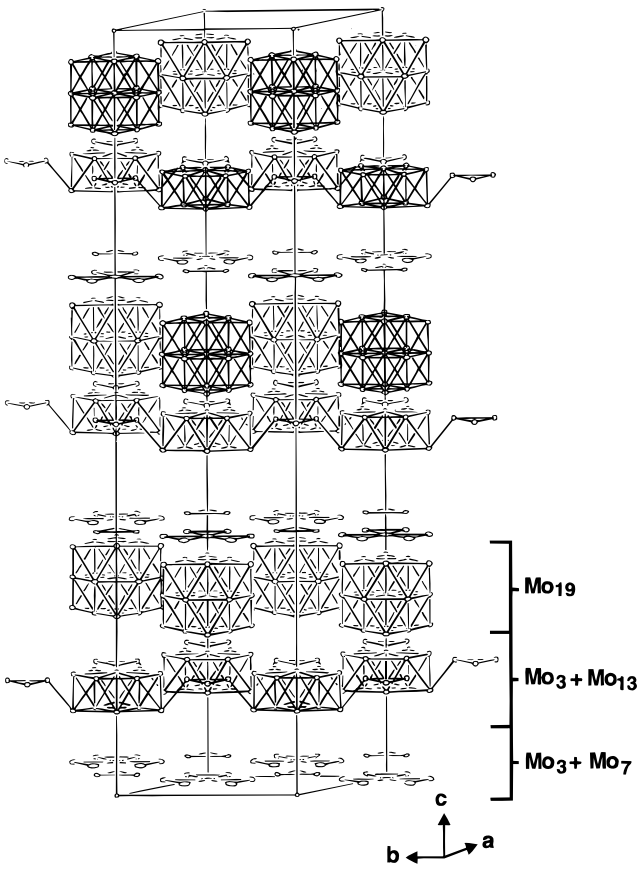

Figure 3. Arrangement of the four different Mo clusters within the hexagonal unit-cell.

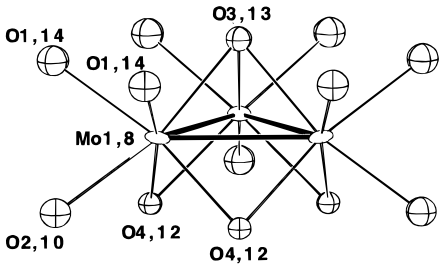

Figure 4. Mo_3 cluster with its oxygen environment. The first numbers correspond to the unit of slab A and the second to the unit of slab C. Ellipsoids are drawn at the 97% probability level.

(R = Sc, Y, In, Sm, Gd, Dy, Ho, Er, Yb),[38−40] $AZn_2Mo_3O_8$ (A = Li, Sc), and $Zn_3Mo_3O_8$.[41] In these compounds, the number of electrons per Mo_3 cluster ranges from six to eight with Mo−Mo distances varying between 2.53 and 2.58 Å, respectively. In $Pr_4Mo_9O_{18}$, the molybdenum atoms Mo(1) form an equilateral triangle in which the Mo−Mo distances are 2.520(2) Å and thus quite close to the 2.53 Å observed in the six-electron cluster $Zn_2Mo_3O_8$. Each molybdenum atom is linked to two other molybdenum atoms and to six oxygen atoms which form a distorted octahedron. Thus, the Mo_3 triangle is surrounded by thirteen oxygen atoms leading to a Mo_3O_{13} unit as represented in Figure 4. The oxygen atoms bridge the edges of the triangle (O(4)), cap the triangular face (O(3)) or are bonded exo to the three Mo vertices of the triangle (O(1), O(2)). In this unit, the Mo−O distances range from 2.046(6) to 2.117(8) Å with an

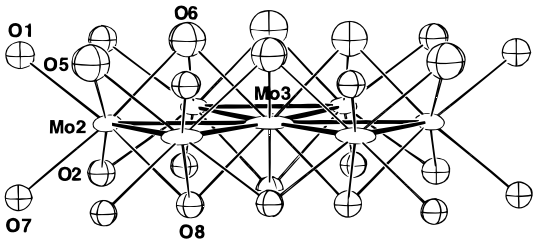

Figure 5. Mo_7 cluster with its oxygen environment (97% probability ellipsoids).

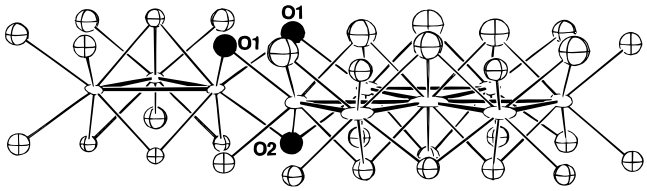

Figure 6. Intercluster bonding via oxygen atoms (in black circles) to form the A slab parallel to the *a*,*b* plane.

average value of 2.07 Å. The second cluster present in the slab A is the planar Mo_7. It may be regarded as a highly distorted hexagonal ring the inside of which is occupied by a seventh molybdenum atom. However, because of the positional disorder of the Mo(3) atom around the center of the hexagonal ring, the new Mo_7 cluster can also be seen as the result of the grouping of one Mo_3 triangle and two Mo_2 dimers. This geometry is particularly original since the only planar clusters known in reduced molybdenum oxides are the Mo_3 triangle and the Mo_4 rhomboïd. The latter aggregate was first observed in the hollandite-related compound $Ba_{1.14}Mo_8O_{16}$.[42] Within the Mo_7 cluster, the coordination of the central Mo(3) atom is extremely rare for a transition metal and, to our knowledge, has only been observed for manganese in $[Mn][Mn_7(THF)_6][Mn(CO)_5]_2$,[43] copper in $[Et_4N]_3[Cu_5Fe_4(CO)_{16}]$,[44] and silver in $[Et_4N]_3[Ag_5\{\mu_2\text{-}Fe(CO)_4\}_2\{\mu_3\text{-}Fe(CO)_4\}_2]$.[45] The hexagon formed by the Mo(2) atoms is distorted with alternate short (2.546(2) Å) and long (2.957(2) Å) distances between them. The central Mo(3) atom is only 0.015 Å from the plane formed by the Mo(2) atoms. Because of the delocalization of the Mo(3) atom around the 3-fold axis, there are three different Mo(2)−Mo(3) distances that are 2.604(6), 2.7668(9), and 2.900(6) Å. The average Mo−Mo distance is 2.75 Å in the Mo_7 cluster. As observed for the Mo_3 cluster, each molybdenum atom is in an octahedral oxygen environment where the oxygen atoms bridge the edges of the hexagon (O(2), O(5)), cap the triangular faces (O(6), O(8)) or are linked in the terminal position to the Mo(2) atoms (O(1), O(7)). The Mo−O distances lie between 1.962(9) and 2.250(9) Å with an average Mo−O value of 2.10 Å. Consequently, there are 24 oxygen atoms surrounding the planar Mo_7 cluster leading to a Mo_7O_{24} unit that is represented in Figure 5. Within this slab, Mo_3 and Mo_7 clusters coexist in equal proportions and share part of their oxygen environment (O(1), O(2)) in such a way as to form layers parallel to the *a*,*b* plane (Figure 6). Because of the 3-fold axis, each Mo_3 triangle has three Mo_7 clusters as neighbors, and *vice versa*. The shortest distance

(38) McCarroll, W. H. *Inorg. Chem.* **1977**, *16*, 3351.
(39) Donohue, P. C.; Katz, L. *Nature* **1964**, *201*, 180.
(40) Kerner-Czeskleba, H.; Tourne, G. *Bull. Soc. Chim. Fr.*, **1976**, 729.
(41) Torardi, C. C.; McCarley, R. E. *Inorg. Chem.* **1985**, *24*, 476.
(42) Torardi, C. C.; McCarley, R. E. *J. Solid State Chem.* **1981**, *37*, 393.
(43) Kong, G.; Harakas, G. N.; Wittlesey, B. R. *J. Am. Chem. Soc.* **1995**, *117*, 3503.
(44) Doyle, G.; Eriksen, K. A.; Van Engen, D. *J. Am. Chem. Soc.* **1986**, *108*, 445.
(45) Albano, V. G.; Azzaroni, F.; Iapalucci, M. C.; Longoni, G.; Monari, M.; Mulley, S.; Proserpio; D. M.; Sironi, A. *Inorg. Chem.* **1994**, *33*, 5320.

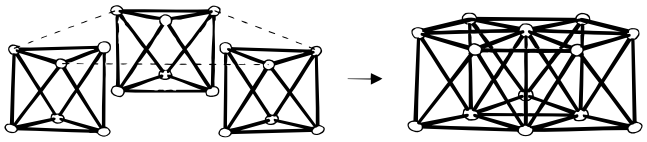

Figure 7. Condensation process for the Mo_{13} cluster.

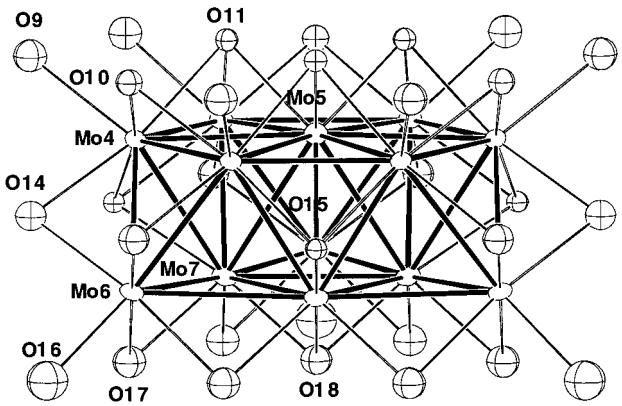

Figure 8. Mo_{13} cluster with its oxygen environment (97% probability ellipsoids).

between these two metallic aggregates is 3.1491(9) Å (Mo(1)−Mo(2)) which excludes any direct Mo−Mo interaction.

The second slab of clusters (C in Figure 2) is characterized by Mo_3 triangles and Mo_{13} clusters that are connected to each other so as to form infinite metallic layers perpendicular to the *c* axis of the hexagonal unit cell. The molybdenum atoms Mo(8) form an equilateral triangle similar to the one described in the A slab. However, the Mo−Mo distances here are slightly longer (2.597(2) Å) and thus quite close to the 2.58 Å observed in the eight electron clusters of $Zn_3Mo_3O_8$. The molybdenum atoms are all in an octahedral environment where the oxygen atoms bridge the edges of the triangle (O(12)), cap the triangular face (O(13)) or are linked in the terminal position to the vertices of the triangle (O(10), O(14)) (Figure 4). The thirteen oxygen atoms that surround the Mo_3 cluster are at 2.033(9) to 2.177(7) Å from the Mo atoms with an average Mo−O distance of 2.10 Å.

The Mo_{13} cluster, which has 3*m* (C_{3v}) symmetry, is particularly original and may be regarded as resulting from the edge-sharing-condensation of three Mo_6 octahedra having the same apex in common, as depicted in Figure 7. This condensation process of the Mo_6 octahedra is not uniaxial as for the previous condensed Mo clusters but can be considered as bidimensional. This new cluster may also be seen as the superposition of two pieces of compact layers, the first one being similar to the Mo_7 cluster previously described and the second corresponding to a Mo_6 supertriangle of order 2 (ν_2 triangle). The Mo−Mo bond distances within the Mo_{13} cluster range from 2.568(1) to 2.860(2) Å with an average value of 2.74 Å and are thus quite comparable to those found in uniaxial condensed Mo clusters. On the other hand, one can notice that the Mo−Mo distances vary only from 2.766(2) to 2.7783(7) Å in the Mo_6 supertriangle while they spread over a wide range (2.568(1)−2.853(1) Å) both in the centered Mo_7 distorted hexagon as well as between the two planes (2.7280(9)−2.860(2) Å). The molybdenum atoms are linked to three (Mo(5)), four (Mo(7)) or five (Mo(4), Mo(6)) oxygen atoms. These bridge the Mo−Mo edges (O(10), O(14), O(17)), cap the triangular Mo faces (O(11), O(15), O(18)) or are bonded exo to the Mo apices of the Mo_{13} polyhedron (O(9), O(16)) leading to the $Mo_{13}O_{31}$ unit shown in Figure 8. The Mo−O bond distances lie between 1.975(8) and 2.169(7) Å with an average value of 2.07 Å. The two units Mo_3O_{13} and $Mo_{13}O_{31}$ share part of their oxygen environment (O(10), O(14)) in such a way as to form planes that are parallel to the *a*, *b* plane. Within this slab, each Mo_{13} is linked through Mo−Mo bonds of 2.808(1) Å (Mo(8)−Mo(6)) to three adjacent Mo_3 triangles and *vice-versa*, leading to a two-dimensional infinite metallic network (Figure 9).

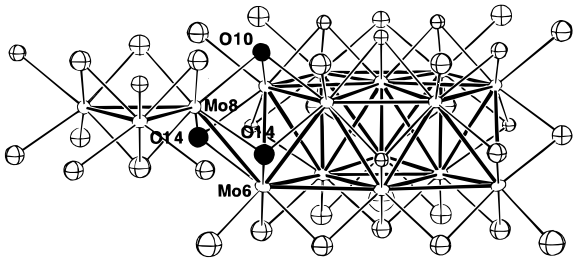

Figure 9. Intercluster bonding via oxygen atoms (in black circles) to form the C slab parallel to the *a*,*b* plane.

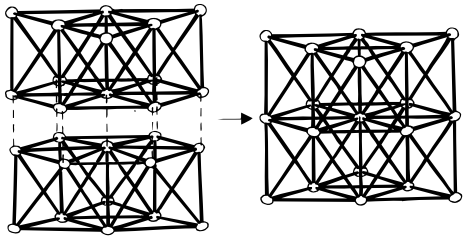

Figure 10. Condensation process for the Mo_{19} cluster.

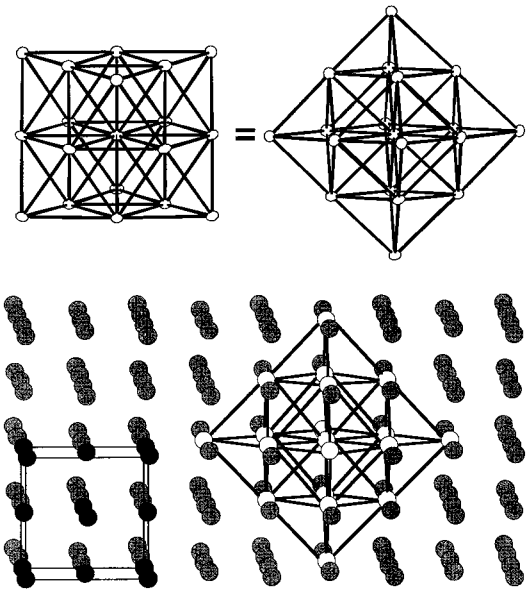

Figure 11. Relationship between the Mo_{19} cluster and the fcc unit cell.

The third and last metallic slab (D in Figure 2) is based on large isolated Mo_{19} clusters having 3*m* (C_{3v}) symmetry. This massive aggregate can be described as the result of the hexagonal-face-sharing of two inverse Mo_{13} clusters as shown in Figure 10, and consequently, as the tridimensional edge-sharing-condensation of six Mo_6 octahedra having one apex in common so that each octahedron shares four edges and five apices with the adjacent ones. A different orientation of this Mo_{19} cluster shown in Figure 11 reveals that this macrocluster is actually an octahedron of order 2 (ν_2 octahedron) and thus constitutes a fragment of an fcc close-packed arrangement of Mo atoms as schematized in Figure 11. It is interesting to note

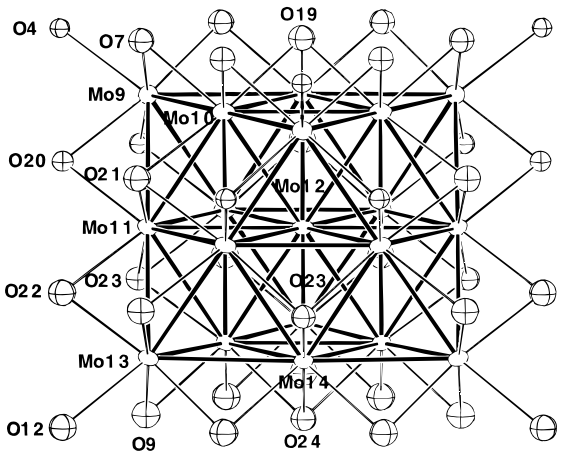

Figure 12. Mo_{19} cluster with its oxygen environment (97% probability ellipsoids).

that, to our knowledge, pure molybdenum metal has only so far been observed in a bcc close-packed arrangement.

Another interesting feature of the Mo_{19} polycluster is the environment of the central atom (Mo(12)) which is not linked to any oxygen atom but to twelve other molybdenum atoms that form a distorted cuboctahedron. This type of metallic cluster, in which a central atom is encapsulated, is much more frequently observed in metal−organic chemistry with palladium,[46] rhodium,[47] or platinum[48] for example. Despite its low symmetry (C_{3v}) with respect to the ideal O_h, the Mo−Mo bond distances are quite homogeneous within this Mo_{19} aggregate and only range from 2.7476(7) to 2.805(2) Å with an average bond distance of 2.78 Å. The latter value is slightly longer than the one observed for pure Mo metal (2.72 Å). It is also interesting to note that the internal centered Mo_7 hexagon is quasiregular with Mo−Mo distances ranging between 2.773(2) and 2.779(2) Å. The other molybdenum atoms are bonded to four (Mo(10), Mo(11), Mo(14)) or five (Mo(9), Mo(13)) oxygen atoms. As for the Mo_{13} aggregate, the oxygen atoms bridge the Mo−Mo edges (O(7), O(9), O(20), O(22)), cap the triangular Mo faces (O(19), O(21), O(23), O(24)) or are bonded exo to the six Mo apices of the ν_2 octahedron (O(4), O(12)). This leads to the $Mo_{19}O_{38}$ unit represented in Figure 12. The Mo−O bond distances lie between 2.004(5) and 2.130(7) Å with an average value of 2.063 Å. The shortest distance between Mo_{19} clusters is about 4 Å which excludes any direct metal−metal interaction.

The eight crystallographically independent rare-earth atoms present in this structure show four different types of environment with coordination numbers in oxygen atoms going from eight to ten, as represented in Figure 13. The four different oxygen environments are all based on pyramids or bipyramids that have a split apex. Pr(3), Pr(4), and Pr(8), which form the B slab (Figure 2), are surrounded by eight oxygen atoms. Pr(5) atoms are connected to nine oxygen atoms and occupy sites between the Mo_3O_{13} and $Mo_{13}O_{31}$ units in the C slab. Pr(2) and Pr(6) atoms, that are ten-coordinate in oxygen, and Pr(1) and Pr(7) atoms, that are eight-coordinate, occupy cavities between the $Mo_{19}O_{38}$ units within the D slabs. The Pr−O distances range from 2.252(5) Å to 3.102(8) Å, as usually observed for the Pr^{3+} cations.[49]

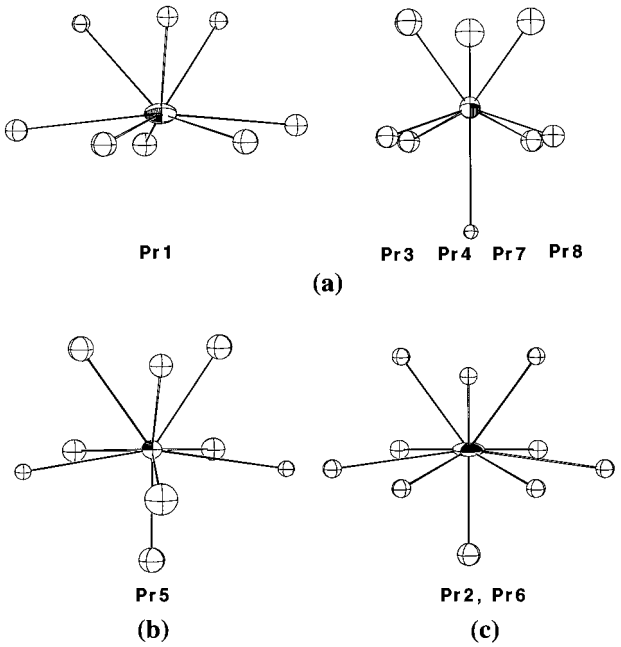

Figure 13. Four different environments observed for the Pr^{3+} ions in $Pr_4Mo_9O_{18}$ (97% probability ellipsoids): (a) CN8, (b) CN9, and (c) CN10.

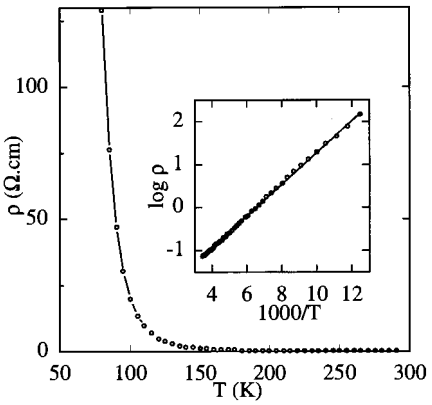

Figure 14. Resistivity of $Pr_4Mo_9O_{18}$ plotted versus temperature. The inset shows the logarithm of the resistivity as a function of inverse temperature.

Electron Count Consideration. From the Mo−O bond lengths, the valences of the 14 crystallographically independent Mo atoms have been calculated using the relationship of Brown and Wu [$s = (d_{Mo-O}/1.882)^{-6.0}$].[50] This yields an average value of +2.66(3), which is in very good agreement with the expected value of +2.67 calculated from the stoichiometry.

Resistivity and Magnetic Properties. Figure 14 shows the crystal resistivity data of $Pr_4Mo_9O_{18}$ in the temperature range 80−290 K. The temperature dependence of the electrical resistivity was carried out on a single crystal (dimens, 0.42 × 0.34 × 0.05 mm^3) in the *a*, *b* plane with a current of 1 μA. $Pr_4Mo_9O_{18}$ is a semiconductor with a resistivity of ca. 8×10^{-2} Ω.cm at room temperature and ca. 130 Ω cm at 80 K. The calculated activation energy extracted from the fit of the log(ρ) versus 1000/*T* plot is 0.08 eV (inset of Figure 14).

Thermic variation of the inverse of the molar magnetic susceptibility clearly shows paramagnetic behavior at high

(46) Mednikov, E. G.; Eremenko, N. K.; Slovokhotov, Y.; Struchkov, L. *J. Organomet. Chem.* **1986**, *C35*, 301.
(47) Albano, V. G.; Ciani, G.; Martinengo, S.; Sironi, A. *J. Chem. Soc., Dalton Trans.* **1979**, 978.
(48) Washecheck, D. M.; Wucherer, E. J.; Dahl, L. F.; Ceriotti, A.; Longoni, G.; Manassero, M.; Sansoni, M.; Chini, P. *J. Am. Chem. Soc.* **1979**, *101*, 6110.
(49) ICSD, *Inorganic Crystal Structure Database*; Gmelin-Institut für Anorganische Chemie und Fachinformationzentrum FIZ Karlsruhe: Germany, 1995.
(50) Brown, I. D.; Wu, K. K. *Acta Crystallogr.* **1976**, *B32*, 1957.

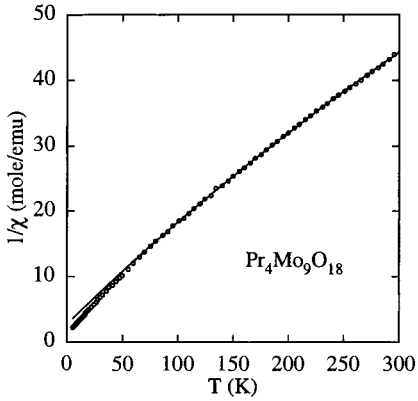

Figure 15. Inverse of the molar magnetic susceptibility as a function of temperature for $Pr_4Mo_9O_{18}$. The solid line is the fitting.

temperatures (Figure 15). Data can be least-squares fit using the modified Curie−Weiss law, $\chi = \chi_o + C/(T - \theta_p)$ over the temperature range 170−300 K. The resulting parameters are $\chi_o = 0.004$ emu/mol, $\theta_p = -16.2$ K, and $C = 1.47$ emu K/mol. The latter value leads to an effective moment $\mu_{eff} = 3.43\ \mu_B$ which is in good agreement with the free-ion value of $\mu_{Pr^{3+}} = 3.58\ \mu_B$.

Conclusions

In summary, $Pr_4Mo_9O_{18}$ is one of the most astonishing compounds containing metal−transition clusters synthesized in solid-state chemistry to date. Apart from the Mo_3 triangle, the Mo_7, Mo_{13}, and Mo_{19} clusters have geometries that are unusual and new to solid-state compounds. The discovery of the latter three clusters is a forerunner of novel geometries for high-nuclearity molybdenum clusters that resulted previously only from linear trans-edge- or -face-sharing condensation of Mo_6 octahedra. Finally, owing to the $Pr_4Mo_9O_{18}$ compound, the appearance of massive condensation of Mo_6 octahedra yields cluster geometries that bring closer together solid-state and metal−organic chemistry.

Acknowledgment. We thank Dr. H. Noël for the collection of the magnetic susceptibility data.

Supporting Information Available: An X-ray crystallographic file for $Pr_4Mo_9O_{18}$, in CIF format, is available on the Internet only. Access information is given on any current masthead page.

IC980500H